Effect of Mass Offset on the Torsional Response in Friction Pendulum Isolated Structures

T.C. Becker
Disaster Prevention Research Institute, Kyoto University, Japan

E.S. Keldrauk, M.W. Mieler & S.A. Mahin
University of California, Berkeley, United States

B. Stojadinovic
IBK, Swiss Federal Institute of Technology (ETH) Zürich, Switzerland

SUMMARY:
Offset of the center of mass in seismically isolated structures can result in large torsional responses. However, in friction pendulum isolators, the horizontal stiffness is directly dependent on the axial load, thus a shift in center of mass leads to a shift in center of rigidity, limiting eccentricity. To examine the effects of shifting the center of mass on a triple friction pendulum (TFP) isolated structure, experimental shake table tests were conducted. The test setup consisted of stacked rigid blocks supported by four TFP bearings. The blocks were restacked between tests to shift the location of the center of mass. Response to cyclic sine-wave input is used to calibrate a numerical bidirectional model of the TFP bearing. The model is then extended to simulate the response of the tested system. Finally, the behavior from both the experimental and numerical models under earthquake loading with varying mass offsets is examined and compared.

Keywords: Isolation, Torsion, Friction Pendulum, Shake Table Testing

1. INTRODUCTION

Mass offset leading to torsion is important to understand especially in isolated buildings where isolation drifts are orders of magnitude larger than drifts in fixed base structures. For this reason isolation codes often include a factor by which the isolation displacement capacity must be increased. However, mass offsets effect elastomeric (rubber) and sliding isolation systems differently. The horizontal stiffness in rubber bearings is not linearly related on the axial load (although it is dependent on it); thus torsional coupling is expected to occur when the center of mass is offset from the center of the isolation system. Jangid and Kelly (2000) show that the effect of eccentricities in rubber isolated structures is dependent on the torsional frequency of the isolation system.

In sliding isolation systems, such as single or triple friction pendulum bearings, the horizontal force is directly related to the axial load on the bearings. Thus, when mass is offset, the center of rigidity is also offset, resulting in zero eccentricity. This will be explained in detail in Section 3. Earlier studies have been conducted to assess the effects of mass eccentricities on the behavior of single pendulum friction isolators (Zayas et al., 1987; Zayas et al., 1989; Anderson, 2003). In these studies the response of the systems tested tended to have little torsional response about their respective vertical axes. To examine the effects of shifting the center of mass on a triple friction pendulum (TFP), which has a more complex behavior than the single friction pendulum bearing, isolated structure experiments were conducted at the Earthquake Simulation Laboratory at University of California, Berkeley. A numerical model was then used for comparison.

2. EXPERIMENTAL PROCEDURE

The experiments consisted of four concrete mass blocks post-tensioned to a steel frame supported by four identical triple friction pendulum (TFP) bearings. A photograph is given in Fig 2.1; and elevation and plan views are shown in Fig 2.2. The bearings were located 6 feet apart in the X (North-South) direction and 9 feet apart in the Y (East-West) direction. The concrete mass blocks weighed 16.9 kips each. TFP bearings (Fig 2.3) consists of four stacked spherical sliding surfaces which creates an isolation bearing with multiple stages. The TFP bearing gradually softens as the friction coefficients of the different sliding surfaces are reached and then gradually hardens as the displacement capacities of the different sliders are reached. A detailed description of the TFP bearing can be seen in Fenz and Constantinou (2007a, 2007b) and Morgan and Mahin (2008). The properties of the TFP bearings used in this study are given in Table 2.1.

To observe the effect of mass offsets in the system, three model configurations were tested, each corresponding to a different level of horizontal mass offset (i.e. number of offset concrete blocks) in the Y direction. The first configuration has all mass block centered over the isolation bearings and corresponds to the case of zero horizontal mass eccentricity in both X and Y directions as depicted in Fig 2.2. Note the orientation of positive X and Y directions in Fig 2.2(a). The second configuration has the top two mass blocks offset by 3 feet in the positive Y direction. The third configuration, shown in Fig 2.1, has three mass blocks offset by 3 feet in the positive Y direction. These offsets result in center of mass offsets of 0, 17% and 25% of the distance between the bearings in Y direction respectively for the three configurations.

Each configuration was subjected to seven scaled 3-component earthquake records. These seven records were compiled and scaled by Jack Baker (personal communication 2009) for the design of the Berkeley Art Museum located in Berkeley, CA. They reflect the types of earthquakes expected at a site in close proximity to a major fault (in this case the Hayward Fault). Each motion had a different acceleration amplitude scale to match the site demands. The rigid mass model was assumed to be a simple representation of a nuclear power plant. To do this a length scale of 19.7 was assumed. The time steps of the ground motions records were reduced by $\sqrt{19.7}$ accordingly. Table 2.2 summarizes the acceleration amplitude scales and the peak ground displacements (PGD) in the X and Y directions

Figure 2.1. Rigid block experimental set-up with offset center of mass at the UC Berkeley Earthquake Simulator Laboratory

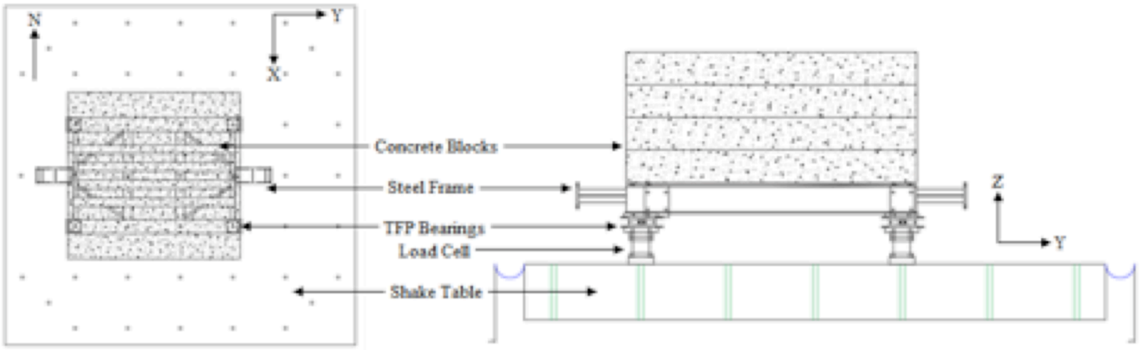

Figure 2.2. Experimental setup elevation and plan views

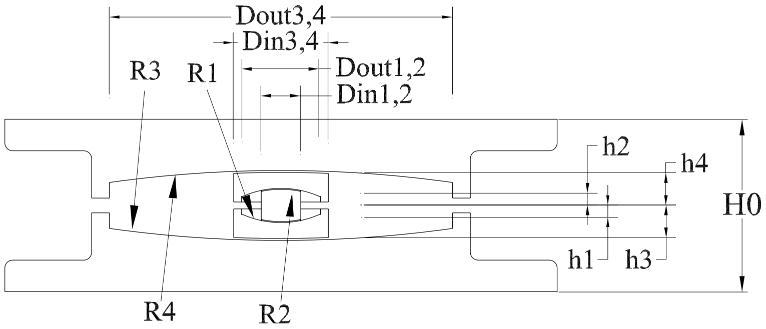

Figure 2.3. Geometry of triple friction pendulum bearings

Table 2.1. TFP bearing properties used in offset block experiment

	Surface 1	*Surface 2*	*Surface 3*	*Surface 4*
R (in)	6	6	18.64	18.64
μ	0.048	0.048	0.1	0.1
D_{out} (in)	3.2	3.2	8.5	8.5
D_{in} (in)	2	2	4	4
h (in)	0.75	0.75	1.25	1.25

Table 2.2. Source records and associated peak ground displacements for the offset block experimental tests

Source Record	*Acceleration Amplitude Scale*	*Peak Ground Displacement (in)*	
		X	*Y*
Duzce, Turkey	1.6	1.347	1.651
Erzincan, Turkey	1.4	0.774	0.614
Imperial Valley, El Centro 7	1.2	0.591	1.073
Imperial Valley, El Centro Differential Array	1.8	1.650	0.505
Landers, California	1.8	9.460	2.510
Loma Prieta, California	1.1	1.447	0.538
Superstition Hills, California	1	1.050	0.310

for the motions used in the experiments. Additionally, the 2 and 3-block models underwent sine wave tests of increasing amplitude at a variety of excitation frequencies. Data from sine wave tests was used to calculate the friction coefficients of the surface of the bearing, given in Table 2.1.

Eigthy-six channels of data were used to capture the behavior of the table and model during testing. Each bearing had a load cell directly underneath to record axial loads, moments and shear forces in the bearings. Accelerometers were used to measure accelerations at the table, frame and top of mass levels. Global frame and local isolator displacements were measured using wire potentiometers and direct current displacement transducers.

3. ANALYTICAL ECCENTRICITY

For the setup described above, the shift in the center of mass with n blocks offset (out of N total) is equal to

$$\Delta\text{CoM}=\frac{nM\delta}{NM} \tag{3.1}$$

where δ is the displacement offset of the blocks and M is the mass of each block assumed to be the same for all blocks. The blocks weighed 16.9 kips each. The steel support frame had a small weight (approximately 1 kip) compared to the blocks and is ignored in the discussion below. The shift of the center of mass with respect to the geometric center of the isolator bearings is 0, 17% and 25% of the longest length between the bearings for the three setups.

To understand the effect of the shift in center of mass, the effect on the eccentricity of the system needs to be examined. The eccentricity is defined as the distance between the center of mass and the center of rigidity. However, in friction pendulum isolators, the horizontal stiffness of the bearings is directly dependent on the axial load, thus a shift in center of mass leads to a shift in center of rigidity. From statics, the axial force on the isolators on the East and West side of the specimen is

$$\begin{aligned} A_{East} &= \frac{1}{2}\frac{NW\,{}^{d}\!/\!_{2}+nW\delta}{d} \\ A_{West} &= \frac{1}{2}\frac{NW\,{}^{d}\!/\!_{2}-nW\delta}{d} \end{aligned} \tag{3.2}$$

respectively, where W is the weight of each block and d is the distance between the isolators in the Y direction, which for the set-up was 9 feet. Ignoring pressure, velocity or temperature effects on friction properties, all four bearings have the same normalized backbone behavior. The stiffness in each bearing is simply the normalized backbone stiffness, referred to here as k, multiplied by the axial load on the bearing. When three of the four concrete blocks are shifted 3 feet, approximately 75% of the total weight is supported by the two Eastern bearings. The shift in the center of rigidity can be found as

$$\Delta CoR = \frac{A_{East}k*\left({}^{d}\!/\!_{2}\right)+A_{West}k*\left(-{}^{d}\!/\!_{2}\right)}{A_{East}k+A_{West}k} \tag{3.3}$$

Plugging in Eqn. 3.2, this reduces to

$$\Delta\text{CoR}=\frac{nW\delta}{NW} \tag{3.4}$$

which is equal to the shift in the center of mass in Eqn. 3.1. The eccentricity is defined as the distance between the center of mass and the center of rigidity

$$e = \Delta CoM - \Delta CoR \tag{3.5}$$

Thus, offsetting the mass does not result in any eccentricity. The same argument can be done for all stages of TFP behavior so long as all bearings are on the same stage and axial loads are distributed according to static gravity considerations for the offset position.

Thus, torsional response during earthquake loading is only expected (1) when bearings are on different stages of behavior (have different k values), (2) when the bearing loads are not distributed according to the static equilibrium resulting in Eqn. 3.2. The first situation is possible if different types of bearings were used in the specimen, if bearings experience substantially different pressure, temperature or velocity conditions or if bearings undergo different horizontal displacements due support flexibility or torsional response. The latter situation is likely due to the presence of overturning moments during earthquake excitations acting on the rigid block. In this case, the distribution of axial loads in the bearings fluctuates to maintain equilibrium under the added overturning moments, shifting the instantaneous center of rigidity away from the center of mass. Almazan and De la Llera (2003) found that, in symmetric structures, torsion due to overturning moments was dependent on the aspect ratio of the structure, but the increase in displacements at the isolation level due to torsion remained below 5%. Thus, the amount of torsion a rigid block about a vertical axis is expected to be small under earthquake loading if the bearings are acting on the same stage (likely if there is little torsion) and if the fluctuation of axial load in the bearing due to transient overturning moments is small compared to the axial load due to gravity and vertical excitations. The alignment of the center of mass with the center of rigidity does not preclude torsional response under eccentrically applied external loads such as missile impacts.

4. NUMERICAL MODEL

The TFP bearing model developed by Becker and Mahin (2012) was implemented to simulate the experimental set-up. Friction coefficients given in Table 2.1 were found using unidirectional sine wave tests. For the bearings used in this set of experiments, the friction coefficients for the outer two surfaces were found to be identical. Each of the four bearings was modeled separately, all with the same bearing properties. The bearings were assumed to be rigidly linked. Friction pendulum bearings exhibit hysteretic damping and no additional viscous damping was added in the model.

For each earthquake motion and model configuration, the recorded table motion from the corresponding experiment was used as input. *X, Y,* and *Z* acceleration components were input to the model. The axial loads on each bearing were different and continually fluctuated due to vertical acceleration as well as overturning moments in both the *X* and *Y* directions. Axial loads on the bearing were recalculated at each time step. However, because the TFP model used does not model bearing uplift, the bearings were not allowed to go into tension. The tangent horizontal and rotational stiffnesses of the system were compiled from the *X* and *Y* stiffnesses of the four bearings considering their deformed configuration using the appropriate transformation matrices.

When translated in the horizontal direction, TFP bearings increase in height, for the bearings used in these tests the height at maximum displacement increases by roughly 0.35 inches. This change in height must cause a vertical acceleration. In calculating the axial loads on bearings it was decided that the change in vertical loads due to the change in height would not be added. Small errors (0.001 inches) in calculating heights cause large acceleration spikes that are not present in experimental data. To verify if this assumption was valid, vertical accelerations measured at the shake table and frame level (above the isolators) were compared. It was found that the vertical accelerations measured above and below the isolation plane matched well without adding vertical accelerations coming from the TFP bearings.

5. RESULTS

Figures 5.1 and 5.2 show experimental and numerical results for the axial loads, and *X* (North-South) direction bearing hysteresis for the East and West bearings measured during the Erzincan, Turkey earthquake excitation for the three offset mass configurations. The numerically calculated axial load is a good match to the experimental values. As described in Section 3, the force in the bearings is dependent on the axial load on them. Thus East bearings show greater forces than West bearings when the mass is offset in the East direction. Figures 5.1 and 5.2 also show the theoretical eccentricity given by Eqn. 3.5 for the experimental tests. To this, the center of rigidity is found at each time step using Eqn. 3.3. Thus, this calculation assumes that all bearings are on the same stage of travel. In the numerical model (Fig 5.2) oscillations in axial load and eccentricity are seen after the motion ends. This is due to the absence of viscous damping in the model mentioned in Section 4. Once the motion ends, the TFP bearings return to a force near zero. However, if the bearings are not yielding (below 4.8%g in the case of these bearings) there is no hysteretic damping in the bearings. However, during earthquake motion we see that the numerical model closely matches the eccentricity calculated from the experiments. No significant difference in eccentricity is observed between the three offset mass cases in either numerically or experimentally.

Accordingly, the experimental tests showed that the effect of offsetting the center of mass even by relatively large amounts does not have a significant influence on behavior in rigid TFP isolated structures under bidirectional earthquake support excitation. The hysteresis loops shown in Figs 5.1 and 5.2 for the bearings on the East and West side of the experiment are similar regardless of the offset of the mass blocks. Displacement orbits and rotation time histories measured at the original center of mass (before blocks were offset) for three earthquake excitations are shown in Fig 5.3 for the experimental and numerical runs. Displacement orbits are similar for all offset cases. Interestingly, although all rotations remained small, the peak rotation values seen in the experimental tests decreased with increase in mass block.

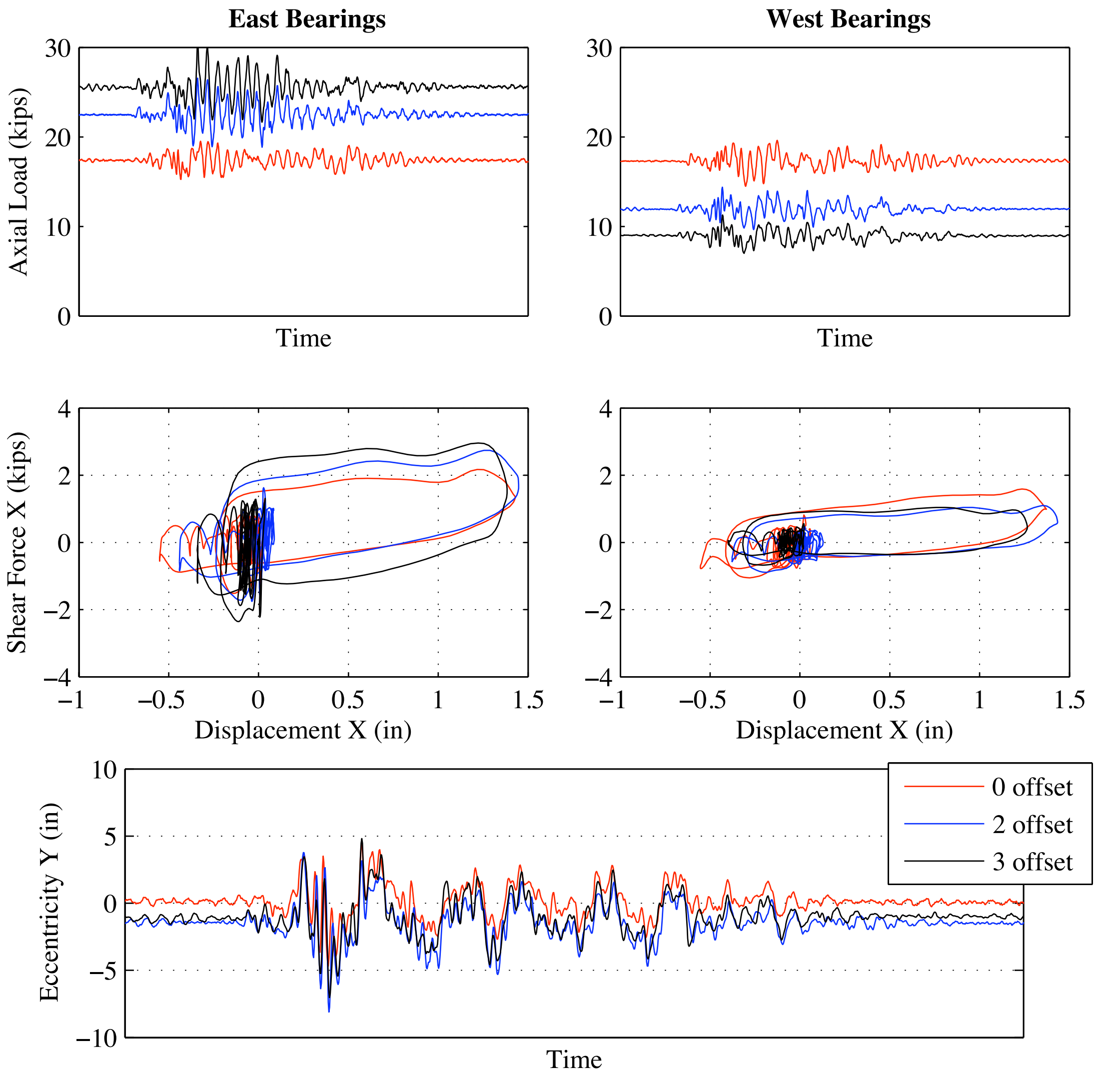

Figure 5.1. Axial loads, *X* direction hysteresis loops and eccentricity for Erzincan earthquake excitation with 0, 2 and 3 blocks offset from experimental data

In general, the numerical orbits show that the bearings do not recenter; this is a characteristic of hysteretic models. However, in the experimental results bearings recentered or returned closer to zero. Thus, the residual rotation at the end of the motion tended towards zero. As the TFP bearings modelled in numerical analyses did not recenter, the residual rotations were larger than in experimental results. However, the numerical analyses resulted in rotation values of the same magnitude as in the experimental results.

Table 5.1 lists the maximum displacements of the model for all ground motions and mass configurations, found from both the experimental results and from the numerical model, in the *X* direction measured at the geometric center of the bearings and at the bearing that experiences the largest displacement in the *X* direction. The displacements are normalized by the maximum table displacement in *X* direction for the corresponding motion. The percent increase in displacement is also listed. Increases *X* direction are listed because for an isolation system that did not have horizontal stiffness linearly dependent on axial load, this would be the direction under which torsion would increase displacement at the extremities of the model. Values for the increase in displacements show that, except for two excitations, the model tends to under predict the increase seen. However, the order of magnitude of the increase is correct and for all earthquakes increases in displacement at the extremities of the model were small. Both the experimental results and the numerical model show no relationship between mass offset and increase in displacement at the model extremities.

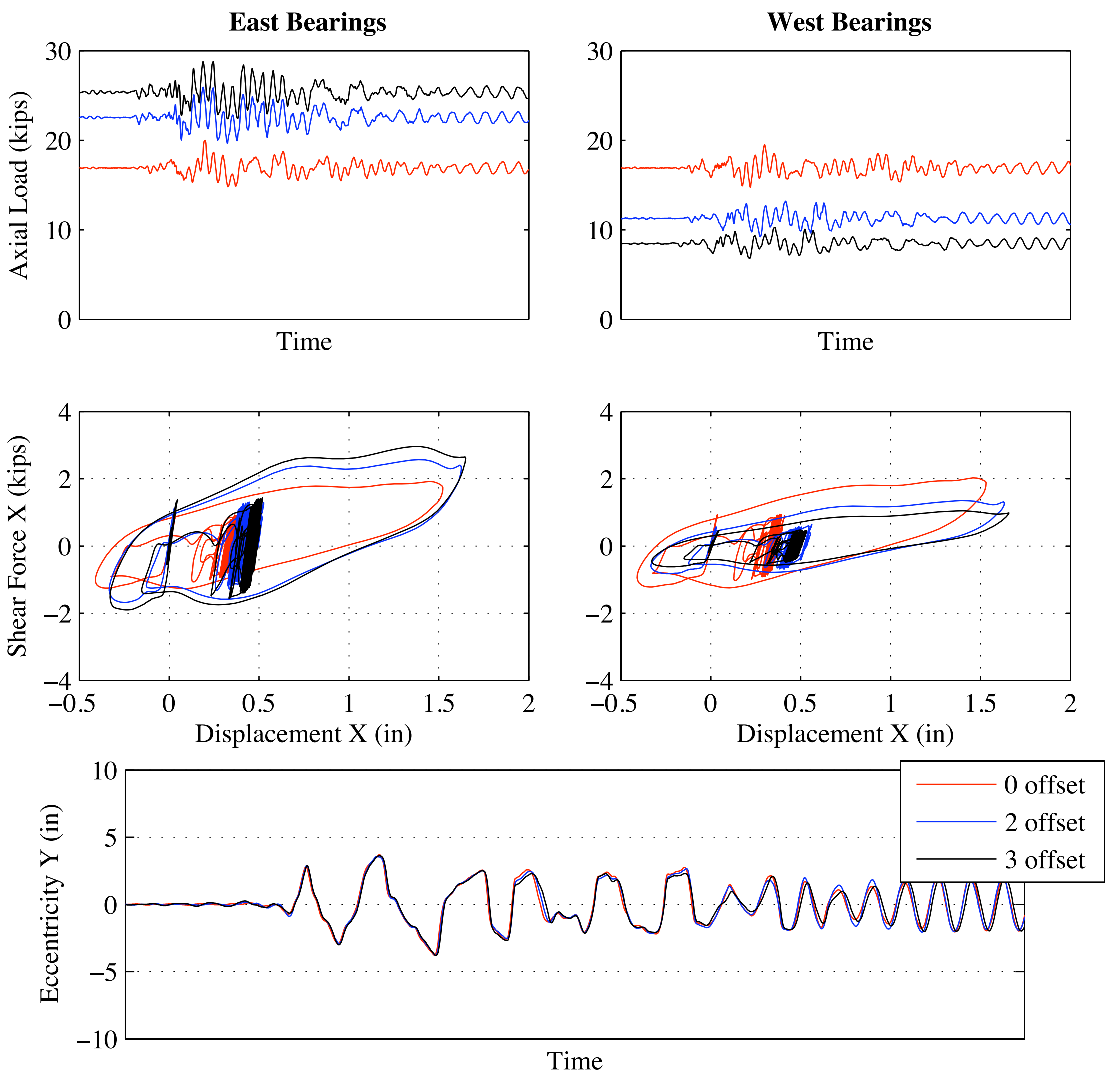

Figure 5.2. Axial loads, *X* direction hysteresis loops and eccentricity for Erzincan earthquake excitation with 0, 2 and 3 blocks offset from numerical simulation

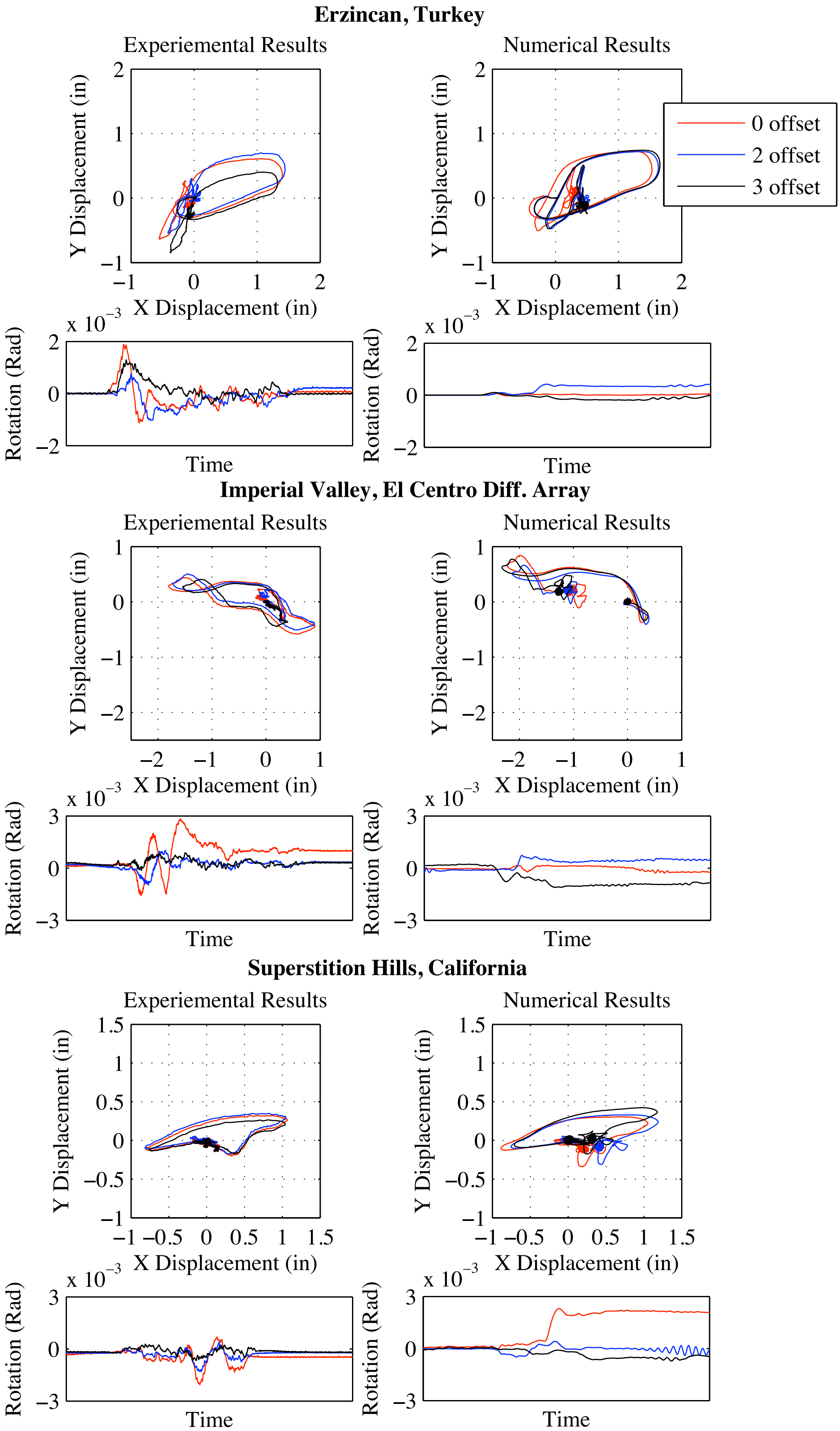

Figure 5.2. Numerically and experimentally measured displacement orbits and rotation time histories for three different earthquake excitations with 0, 2 and 3 blocks offset

Table 5.1. Maximum *X* displacement measured at the geometric center of the specimen and at the bearing with largest displacement normalized to peak table *X* displacement

Source Record	*# Blocks Offset*	*Experimental Results*			*Numerical Results*		
		Max Center Disp X	*Max Bearing Disp X*	*% Inc*	*Max Center Disp X*	*Max Bearing Disp X*	*% Inc*
Duzce, Turkey	0	1.71	1.91	**12**	0.88	0.88	1
	2	1.73	1.87	8	0.85	0.85	0
	3	1.30	1.35	4	0.98	0.98	0
Erzincan, Turkey	0	1.84	1.88	2	2.00	2.01	0
	2	1.92	1.92	0	2.16	2.17	0
	3	1.76	1.84	5	2.20	2.20	0
Imperial Valley, El Centro Array #7	0	1.77	1.84	4	1.08	1.11	2
	2	1.18	1.25	6	1.93	1.95	1
	3	1.44	1.55	8	1.32	1.32	1
Imperial Valley, El Centro Diff. Array	0	1.59	1.64	3	1.97	1.97	0
	2	1.54	1.56	0	1.90	1.91	0
	3	1.37	1.39	1	2.06	2.09	2
Landers California	0	1.06	1.08	2	1.10	1.13	3
	2	1.05	1.06	0	1.12	1.20	7
	3	1.00	1.02	3	1.10	1.15	5
Loma Prieta, California	0	1.20	1.30	8	1.46	1.46	0
	2	1.29	1.30	0	1.45	1.45	0
	3	1.24	1.27	2	1.52	1.52	0
Superstition Hills, California	0	1.51	1.63	8	1.49	1.62	9
	2	1.49	1.57	5	1.69	1.72	2
	3	1.46	1.50	3	1.65	1.66	1

Many isolation design codes specify increases in displacement due to torsional response. The ASCE (2005) code gives total displacement D_T due to torsion as

$$D_T = D\left[1 + y\frac{12e}{b^2 + d^2}\right] \tag{5.1}$$

where D is the displacement at the center of rigidity, e is defined as in Eqn. 3.5, b and d are the dimensions of the structure and y is the distance form the center of rigidity the element of interest. The term for e in the code includes an addition for accidental torsion of 5% of the longest plan dimension of the structure. If, for the experiments presented here, this is taken to be 5% of 9 feet, Eqn. 5.1 results in a 20% increase in displacement of for the corner bearings. As seen in Table 5.1, increase in displacement from the geometric center of the bearings to the bearing that underwent the greatest amount of displacement remained well under 20% for all excitations.

6. CONCLUSIONS

This study consisted of experimental and numerical studies of a triple friction pendulum (TFP) bearing supported rigid mass block in which the center of mass was offset from the center of the bearings by various degrees. Through simple calculations it was shown that the offset of center of mass results in an equal offset of the center of rigidity and thus does not result in eccentricity. However, small amounts of eccentricity are to be expected due to changes in load distribution due to overturning moments in the structure. Experimental and numerical results both confirmed that torsional response of the system was minimal and resulted in increases in displacement demand for isolators at the extremities of the model that were far below the code specified increases meant to account for accidental torsion. Although the amount of load fluctuation due to overturning moment is depended on the geometry of the specific project, the tendency of the center of mass and center of rigidity to coincide for most loading conditions is a benefit for friction pendulum isolation systems with significant mass eccentricities. This study shows that seismic isolation with triple friction pendulum bearings could be a solution for structures with large non-uniform mass distributions.

AKCNOWLEDGEMENTS

This paper is based upon work supported by the National Science Foundation under Grant No. CMMI-0724208 and the Department of Energy under Grant No. DE-FG07-08ID14923. Any opinions, findings, and conclusions expressed here are those of the authors and do not necessarily reflect the views of the National Science Foundation or the Department of Energy. Appreciation is given to Earthquake Protection Systems for providing the bearings used in the experiments.

REFERENCES

Almazan, J.L. and De la Llera, J.C. (2003). Accidental torsion due to overturning in nominally symmetric structures isolated with FPS. *Earthquake Engineering Structural Dynamics* **32**: 919-948.

American Society of Civil Engineers (2005). *Minimum Design Loads for Buildings and Other Structures.* Standard ASCE/ SEI 7-05, Reston, VA.

Anderson, E.L. (2003). *Performance-Based Design of Seismically Isolated Bridges.* Doctoral Dissertation, University of California, Berkeley.

Becker, T.C. and Mahin, S.A. (2012). Experimental and analytical study of the bi-directional behavior of the triple friction pendulum isolator. *Earthquake Engineering Structural Dynamics* **41**: 355-373.

Fenz, D.M. and Constantinou, M.C. (2007a). Spherical sliding isolation bearings with adaptive behavior: Theory. *Earthquake Engineering and Structural Dynamics* **37**(1): 163-183.

Fenz, D.M. and Constantinou, M.C. (2007b). Spherical sliding isolation bearings with adaptive behavior: Experimental verification. *Earthquake Engineering and Structural Dynamics* **37**(2): 185-205.

Jangis, R.S. and Kelly, J.M. (2000). Torsional displacements in base-isolated buildings. *Earthquake Spectra* **16**(2): 443-454.

Morgan, T.A. and Mahin, S.A. (2008). The optimization of multi-stage friction pendulum isolators for loss mitigation considering a range of seismic hazard. *Proceedings of the 14th World Conference on Earthquake Engineering*. Beijing, China.

Zayas, V.A., Low, S.S., Mahin, S.A. (1987). *The FPS Earthquake Resisting System.* Report No. EERC 87-01. Earthquake Engineering Research Center, Berkeley, CA.

Zayas, V.A., Low, S.S., Bozzo, L. Mahin, S.A. (1989). Feasibility and Performance Studies on Improving the Earthquake Resistance of New and Existing Buildings Using the Friction Pendulum System. Report No. EERC 89-09. Earthquake Engineering Research Center, Berkeley, CA.